

Enhancement Control Concept of Grid Power Transmission Limits During Day And Night Using PV-Solar Farm as STATCOM

Chinnareddigari Nandeesh Reddy¹, A. Mahesh Kumar Reddy²

¹PG Student, Dept. of EEE, Sri Sai Institute of Technology & Science, Rayachoty.

²Assistant Professor, Dept. of EEE, Sri Sai Institute of Technology & Science, Rayachoty.

Abstract:

This project presents a novel concept of utilizing a photovoltaic (PV) solar farm inverter as STATCOM, called PV-STATCOM, for improving stable power transfer limits of the interconnected transmission system. The entire inverter rating of the PV solar farm, which remains dormant during night time, is utilized with voltage and damping controls to enhance stable power transmission limits. During daytime, the inverter capacity left after real power production is used to accomplish the aforementioned objective. Transient stability studies are conducted on a realistic single machine infinite bus power system having a midpoint located PV-STATCOM using MATLAB simulation software. The PV-STATCOM improves the stable transmission limits substantially in the night and in the day even while generating large amounts of real power. Power transfer increases are also demonstrated in the same power system for 1) two solar farms operating as PV-STATCOMs and 2) a solar farm as PV-STATCOM and an inverter-based wind farm with similar STATCOM controls. This novel utilization of a PV solar farm asset can thus improve power transmission limits which would have otherwise required expensive additional equipment, such as series/shunt capacitors or separate flexible AC transmission System controllers.

Keywords- photovoltaic system, STATCOM, Grid power, Transmission limits.

1. Introduction

These days power frameworks are muddled systems. They have many creating stations and burden focuses that are interconnected through force transmission lines. Power is produced and supplied to shoppers by means of transmission and dissemination arrangements and contributes a noteworthy partake in the shopper markets of the world. Power frameworks of the present day time are more solid and serve client load with no intrusion in utility voltage [1-2]. Era offices ought to have the ability to create obliged energy to take care of the client demand. The mass force created must be transported through transmission frameworks more than a long separation without over warming or imperiling framework strength. It is the obligation of the conveyance framework to convey power to every client's administration passage [3]. In the setting of dependability era, transmission, and conveyance frameworks are comprised of a few subsystems as recorded in Table 1. A disentangled portrayal of a general force framework alongside its sub-frameworks is demonstrated in Fig. 1 could make DG clean vitality a piece of a more expanded future.

TABLE 1: Electric power systems and their subsystems

I.No.	Systems	Subsystems
1	Generation	Generation plants / Generation substations
2	Transmission	Transmission line/ Transmission substations/ switching stations Sub-transmission systems
3	Distribution	Distribution substations Primary distribution systems Dispersed distribution transformers Secondary distribution systems

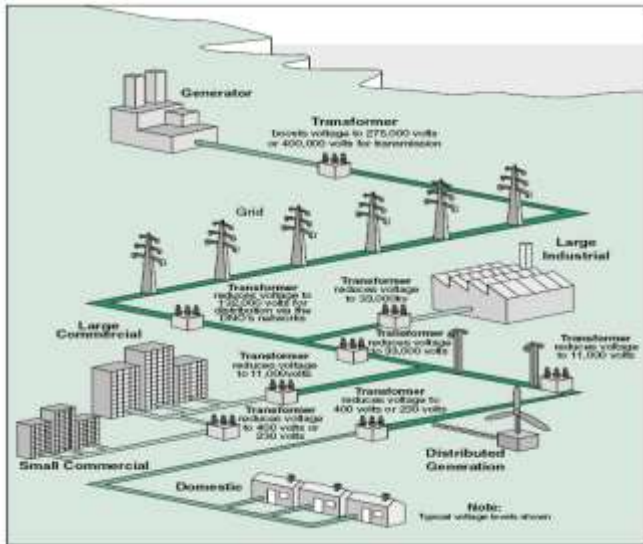


Figure 1: Schematic Diagram Of Overall Power System Network

Electrical Power Generation is commanded by huge generators that are remote from clients and in like manner, supply energy to end clients through a system of transmission and conveyance lines. Be that as it may, new advancements and approach choices are gradually switching the decrease in neighborhood era.

Generally, focal plants have been a vital piece of the electric lattice, in which substantial creating offices are particularly found either near to assets or generally situated a long way from populated burden focuses. These, thusly, supply the customary transmission and circulation (T&D) matrix that conveys mass energy to load focuses and from that point to buyers [4-5]. These were produced when the expenses of transporting fuel and incorporating producing advancements into populated regions far surpassed the expense of creating T&D offices and duties. Focal plants are normally intended to exploit accessible economies of scale in a site-particular way and are manufactured as "erratic," custom tasks.

For instance, coal force plants are constructed far from urban areas to keep their overwhelming air contamination from influencing the masses. Also, such plants are frequently manufactured close collieries to minimize the expense of transporting coal. Hydroelectric plants are by their inclination restricted to working at destinations with the adequate water stream [6-8]. Low contamination is an essential point of interest of consolidated cycle plants that smoulder normal gas. The low contamination allows the plants to be sufficiently close to a city to give region warming and cooling. Circulated vitality assets are mass-created, little, and less site-particular.

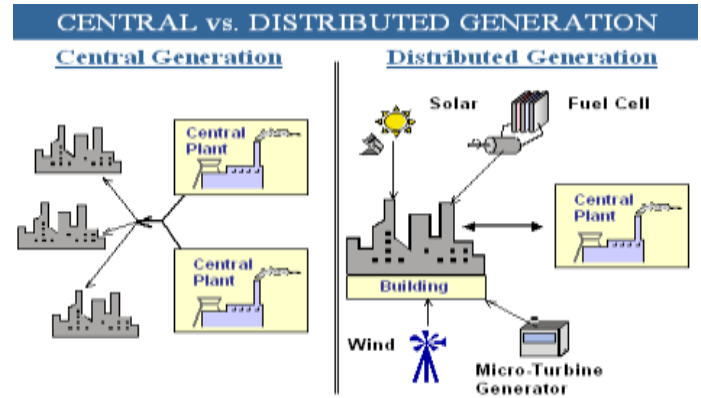


Figure 2: Central Vs Distributed Generation

The Fig. 2 shows the central vs distributed generation. In Dispersed era (or DG) for the most part alludes to little scale (normally 1 kW – 50 MW) electric force generators that deliver power at a site near to clients or that are fixed to an electric circulation framework. Appropriated generators incorporate, however, are not constrained to synchronous generators, incitement generators, responding motors, small scale turbines (burning turbines that keep running on high-vitality fossil powers, for example, oil, propane, normal gas, gas or diesel), ignition gas turbines, energy units, the sun powered photovoltaic's, and wind turbines.

1.1 Literature Survey

Power Quality of grid-connected wind turbines with DFIG and their interaction with the grid

Two control plans are actualized in the created lattice associated wind turbine model: speed control and pitch control. The pace control plan is made by two vector control plans composed individually for the rotor-side and network side PWM voltage source converters. Course control is utilized as a part of the vector-control plans. Two outline techniques, pole placement, and inside model control, are connected for planning the PI-controllers in the vector-control plans. The pitch control plan is utilized to direct the streamlined force from the turbine. The exhibitions of the control plans, individually current control circles, power control circles, DC-join voltage control circle and pitch control circle, are represented, which meet the configuration necessities. Reproduction results demonstrate that the wind turbine is equipped for giving tasteful consistent state and element exhibitions, which makes it conceivable that the wind turbine model can be connected to concentrate on the force quality issues of such sort of lattice associated wind turbines and their collaboration with the framework.

Gleam discharge of wind turbines amid nonstop operation

This anticipates presents an investigation and the demonstrating of the gleam emanation of wind turbines. Estimations contrasted and universal principles are talked about. The paper focuses on the hypothetical parts of the flash calculation, wind turbine attributes and the era of glimmer amid constant operation of wind turbines.

Examination of the gleam discharge by framework associated wind turbines

Wind turbines associated with electrical frameworks may influence impressively the nature of the supply, because of the fluctuating character of their yield power. An imperative impact from their association is the quick variances of the supply voltage, for the most part alluded to as "glint". In this paper, an examination is introduced of the gleam discharge levels from a network associated wind turbine, utilizing a nitty gritty PC reproduction model.

The outcomes incorporate an investigation of the reliance of the glint on the wind attributes (mean worth and turbulence power), network parameters (cut off and impedance edge) and the kind of wind turbine (consistent or variable pace).

Glint study on variable velocity wind turbines with doubly bolstered actuation generator

Lattice associated wind turbines may deliver glint amid persistent operation. This project shows a re-enactment model of an MW-level variable pace wind turbine with a doubly encouraged prompting generator created in the reproduction instrument of PSCAD/EMTDC. Flash emanation of variable pace wind turbines with doubly sustained incitement generators is explored amid consistent operation, and the reliance of glint outflow on mean wind speed, wind turbulence power, cut off of lattice and framework impedance point are broke down. A correlation is finished with the settled velocity wind turbine, which prompts a conclusion that the components said above to have diverse impacts on gleam outflow contrasted and that on account of the altered rate wind turbine. Gleam relief is acknowledged by yield receptive force control of the variable velocity wind turbine with doubly bolstered impelling generator. Re-enactment results demonstrate the wind turbine yield receptive force control gives a powerful intends to gleam relief paying little mind to mean wind speed, turbulence force and short out limit proportion.

2. Photovoltaic Inverter

2.1. Photovoltaic Cell and Array Modelling

A PV cell is a simple p-n junction diode that converts the irradiation into electricity. Fig. 3 illustrates a simple equivalent circuit diagram of a PV cell. This model consists of a current source which represents the generated current from PV cell, a diode in parallel with the current source, a shunt resistance, and a series resistance [9].

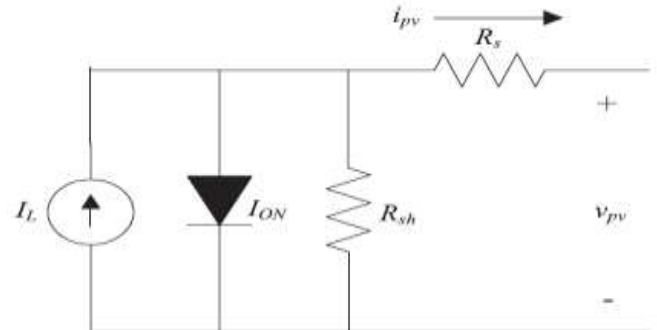


Figure 3: Equivalent circuit diagram of the PV cell

From Fig. 3, the diode current can be expressed as

$$I_{ON} = I_s \left[\exp \left(\frac{q}{AKT_c} (v_{pv} + R_s i_{pv}) \right) - 1 \right] \quad \dots$$

(1)

Where v_{pv} and i_{pv} are the voltage and current of the PV cell output respectively. Other constants and their definitions are shown in Table 2. The output current, generated by the PV cell, can be calculated by applying Kirchhoff's current law, i.e.

$$i_{pv} = I_L - I_s \left[\exp \left[\alpha (v_{pv} + R_s i_{pv}) \right] - 1 \right] - \frac{v_{pv} + R_s i_{pv}}{R_{sh}} \quad \dots (2)$$

the current source output I_L , is related to the solar irradiation and temperature by

$$I_L = \left[I_{sc} + k_i (T_c - T_{ref}) \right] \frac{S}{1000} \quad \dots$$

(3)

where S is the solar irradiation, I_{sc} is the short circuit current, k_i is the short circuit current coefficient, T_c is the cell's operating temperature (in K), and T_{ref} is the reference temperature of the cell.

$$I_s = I_{RS} \left[\frac{T_c}{T_{ref}} \right]^3 \exp \left[\frac{qE_g}{Ak} \left(\frac{1}{T_{ref}} - \frac{1}{T_c} \right) \right] \quad \dots (4)$$

Where I_{RS} is reverse saturation current in the reference temperature and solar irradiation, and E_g is the band gap energy of the PV semiconductor.

TABLE 2: Parameter values of the considered PV model

T_c	Operation Temperature	298C
I_{sc}	Short Circuit Current	3.2A
A	Ideality Factor	1-5
K	Boltzmann's Constant	1.3807×10^{-23}
Q	Electron charge	$1.6022 \times 10^{-19}C$
R	Resistance	0.01ohm

Since the output voltage and current of one PV cell are very low, a combination of series and parallel cells are connected together in order to deliver higher current and voltage. These cells are encapsulated with a transparent material to protect them from harsh environmental conditions and form a PV module. In order to obtain a higher voltage and current for higher power applications, a number of PV modules need to be connected to form a PV array as shown in Fig. 4.

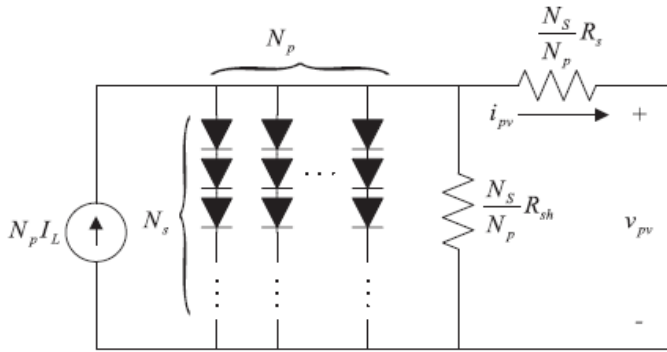


Figure 4: Equivalent circuit diagram of the PV array

If number of PV cells connected in series is N_s and number of PV cells connected in parallel is N_p , then the array output current, i_{pv} can be expressed as

$$i_{pv} = N_p I_L - N_p I_s \left[\exp \left[\alpha \left(\frac{V_{pv}}{N_s} + \frac{R_s i_{pv}}{N_p} \right) \right] - 1 \right] - \frac{N_p}{R_{sh}} \left(\frac{V_{pv}}{N_s} + \frac{R_s i_{pv}}{N_p} \right) \quad \dots(5)$$

2.2 Modelling of Inverter

By considering the inductor currents and capacitor voltage as the state variables of the three-phase grid-connected PV system of Fig. 4, [10,11] the state-space representation of this system will be

$$\begin{aligned} \dot{i}_a &= -\frac{R}{L} i_a - \frac{1}{L} e_a + \frac{v_{pv}}{3L} (2K_a - K_b - K_c) \\ \dot{i}_b &= -\frac{R}{L} i_b - \frac{1}{L} e_b + \frac{v_{pv}}{3L} (-K_a + 2K_b - K_c) \end{aligned}$$

$$\dot{i}_c = -\frac{R}{L} i_c - \frac{1}{L} e_c + \frac{v_{pv}}{3L} (-K_a - K_b + 2K_c) \quad \dots (6)$$

where K_a, K_b and K_c are the switching signals related to each phase of three-phase grid connected photovoltaic system. i_a, i_b, i_c are the output currents from the grid, e_a, e_b, e_c are the output voltages from the grid. On the other hand, by applying KCL to the DC link capacitor node, the state-space equation for capacitor voltage is obtained as

$$\dot{v}_{pv} = \frac{1}{C} (i_{pv} - i_{dc}) \quad \dots (7)$$

Assuming the switching losses and conduction losses of the inverter to be negligible, the input current of the inverter becomes equal to the output current [12] i.e.

$$i_{dc} = i_a K_a + i_b K_b + i_c K_c \quad \dots (8)$$

Which yields,

$$\dot{v}_{pv} = \frac{1}{C} i_{pv} - \frac{1}{C} (i_a K_a + i_b K_b + i_c K_c) \quad \dots (9)$$

Therefore, the state-space model of a loss-less three-phase grid-connected PV system can be represented by

$$\begin{aligned} \dot{i}_a &= -\frac{R}{L} i_a - \frac{1}{L} e_a + \frac{v_{pv}}{3L} (2K_a - K_b - K_c) \\ \dot{i}_b &= -\frac{R}{L} i_b - \frac{1}{L} e_b + \frac{v_{pv}}{3L} (-K_a + 2K_b - K_c) \\ \dot{i}_c &= -\frac{R}{L} i_c - \frac{1}{L} e_c + \frac{v_{pv}}{3L} (-K_a - K_b + 2K_c) \\ \dot{v}_{pv} &= \frac{1}{C} i_{pv} - \frac{1}{C} (i_a K_a + i_b K_b + i_c K_c) \end{aligned} \quad \dots (10)$$

The system described by above equations is a nonlinear time-varying system due to the nature of switching functions and diode current.

2.3 MPPT: (Maximum Power Point Tracking)

Maximum power point tracking (MPPT) is a technique to maximize the energy obtained under all normal operating conditions. The use of MPPT can reduce the cost of energy by making the system more efficient [13-15]. The problem raised by MPPT methods is to automatically find the voltage or current (V_{mp}, I_{mp}) in which a PV array works at

its maximum power point under a certain irradiance and temperature. There are many techniques to realize the MPPT. However, most techniques respond to both irradiance and temperature variations but some responds to constant temperature.

3. Proposed System

The single-line diagrams of two study systems: Study System 1 and Study System 2 are depicted in Fig.5 (a) and 5 (b), respectively. Both systems are single-machine infinite bus (SMIB) systems where a large equivalent synchronous generator (1110 MVA) supplies power to the infinite bus over a 200-km, 400-kV transmission line. This line length is typical of a long line carrying bulk power in Ontario.

3.1 System Models-I

In Study System 1, a 100-MW PV solar farm (DG) as STATCOM (PV-STATCOM) is connected at the midpoint of the transmission line. In Study System 2, two 100-MVA inverter-based distributed generators (DGs) are connected at 1/3 (bus 5) and 2/3 (bus 6) of the line length from the synchronous generator. The DG connected at bus 6 is a PV-STATCOM and the other DG at bus 5 is either a PV-STATCOM or a wind farm with STATCOM functionality. In this case, the wind farm employs permanent-magnet synchronous generator (PMSG)-based wind turbine generators with a full ac-dc-ac converter. It is understood that the solar DG and wind DG employ several inverters. However, for this analysis, each DG is considered to have a single equivalent inverter with the rating equal to the total rating of solar DG or wind DG, respectively. The wind DG and solar DG are considered to be of the same rating, hence, they can be interchanged in terms of location depending upon the studies being performed.

Fig. 6 presents the block diagrams of various subsystems of two equivalent DGs. All of the system parameters are given.

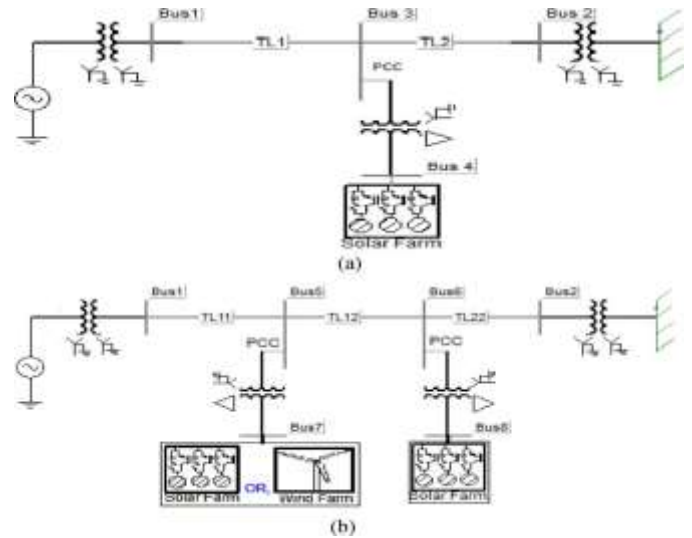


Figure 5: single-line diagram of (a) study system I with a single solar farm (DG) and (b) Study system II with a solar farm (DG) and a solar/wind farm (DG).

The synchronous generator is represented by a detailed sixth order model and a DC1A-type exciter. The transmission-line segments TL1, TL2, TL11, TL12, and TL22, shown in Fig. 5, are represented by lumped pi-circuits. The PV solar DG, as shown in Fig. 6, is modelled as an equivalent voltage-source inverter along with a controlled current source as the dc source which follows the characteristics of PV panels. The wind DG is likewise modelled as an equivalent voltage-source inverter. In the solar DG, dc power is provided by the solar panels, whereas in the full-converter-based wind DG, dc power comes out of a controlled ac-dc rectifier connected to the PMSG wind turbines, depicted as “wind Turbine-Generator-Rectifier (T-G-R).” The dc power produced by each DG is fed into the dc bus of the corresponding inverter, as illustrated in Fig. 6. A maximum power point tracking (MPPT) algorithm based on an incremental conductance algorithm is used to operate the solar DGs at its maximum power point all of the time and is integrated with the inverter controller. The wind DG is also assumed to operate at its maximum power point since this proposed control utilizes only the inverter capacity left after the maximum power point operation of the solar DG and wind DG.

For PV-STATCOM operation during nighttime, the solar panels are disconnected from the inverter and a small amount of real power is drawn from the grid to charge the dc capacitor. The voltage-source inverter in each DG is composed of six insulated-gate bipolar transistors (IGBTs) and

associated snubber circuits as shown in Fig. 6. An appropriately large dc capacitor of size 200 Farad is selected to reduce the dc side ripple. Each phase has a pair of IGBT devices which converts the dc voltage into a series of variable-width pulsating voltages, using the sinusoidal pulse width modulation (SPWM) technique. An L-C-L filter is also connected at the inverter AC side. Fig. 5. Single-line diagram of (a) study system I with a single solar farm (DG) and (b) study system II with a solar farm (DG) and a solar/wind farm (DG).

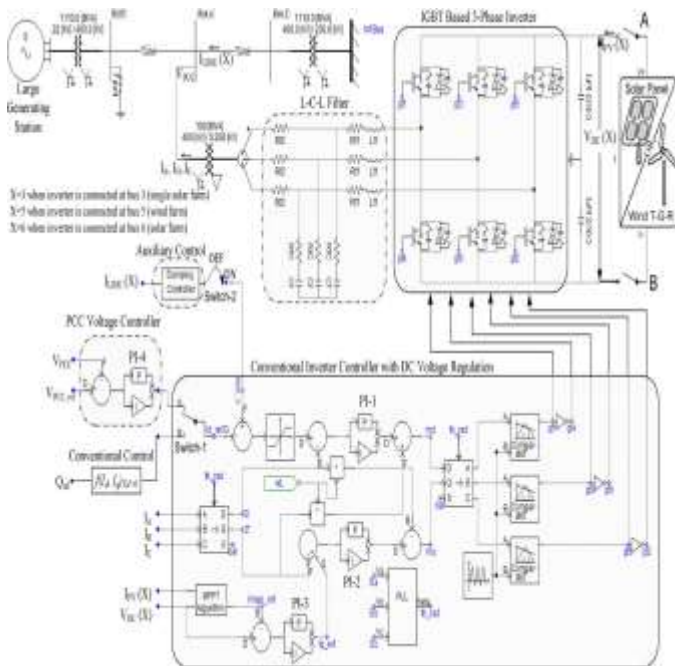


Figure 6: Complete DG (solar/wind) system model with a damping controller and PCC voltage-control system

a) Conventional Reactive Power Control:

The conventional reactive power control only regulates the reactive power output of the inverter such that it can perform unity power factor operation along with dc-link voltage control. The switching signals for the inverter switching are generated through two current control loops in -0 coordinate system. The inverter operates in a conventional controller mode only provided that “Switch-2” is in the “OFF” position. In this simulation, the voltage vector is aligned with the quadrature axis that is, 0, hence, is only proportional to which sets the reference for the upper control loop involving PI1. Meanwhile, the quadrature axis component is used for dc-link voltage control through two PI controllers (PI-2 and PI-3), shown in Fig. 6 according to the set point voltage provided by the MPPT and injects all available real power “P” to the network.

To generate the proper IGBT switching signals (gt1, gt2, gt3, gt4, gt5, gt6), the $-$

components (and) of the modulating signal are converted into three-phase sinusoidal modulating signals and compared with a high-frequency (5-kHz) fixed magnitude triangular wave or carrier signal.

b) PCC Voltage Control:

In the PCC voltage control mode of operation, the PCC voltage is controlled through reactive power exchange between the DG inverter and the grid. The conventional control channel is replaced by the PCC voltage controller in Fig. 6, simply by switching “Switch-1” to the position “A.” Hence, the measured signal at the PCC is compared with the preset reference value and is passed through the PI regulator, PI-4, to generate. The rest of the controller remains unchanged. The upper current control loop is used to regulate the PCC voltage whereas the lower current control loop is used for dc voltage control and as well as for the supply of DG power to the grid. The amount of reactive power flow from the inverter to the grid depends on set point voltage at the PCC. The parameters of the PCC voltage controller are tuned by a systematic trial-and-error method to achieve the fastest step response, least settling time, and a maximum overshoot of 10%–15%. The parameters of all controllers are given in the Appendix.

c) Damping Control:

A novel auxiliary damping controller is added to the PV control system and shown in Fig. 6. this controller utilizes line current magnitude as the control signal. The output of this controller is added with the signal.

The transfer function of this damping controller is expressed as in the transfer function is comprised of a gain, a washout stage, and a first-order lead-lag compensator block. This controller is utilized to damp the rotor-mode oscillations of the synchronous generator and thereby improve system transient stability. The damping controller is activated by toggling “Switch-2” to the “ON” position. This damping controller can operate in conjunction with either the conventional reactive power control mode or with the PCC voltage-control mode by toggling “Switch-1” to position “B” or “A,” respectively. At first, the base-case generator operating power level is selected for performing the damping control design studies. This power level is considered equal to the transient stability limit of the system with the solar farm being disconnected at night. At this operating power level, if a three-phase fault occurs at Bus 1, the generator power oscillations decay with a damping ratio of 5%. The solar farm is now connected and operated in the PV-STATCOM

mode. The parameters of the damping controller are selected as follows.

The washout time constant is chosen to allow the generator electromechanical oscillations in the frequency range up to 2 Hz to pass through the gain, time constants, and is sequentially tuned to obtain the fastest settling time of the electromechanical oscillations at the base-case generator power level through repetitive PSCAD/EMTDC simulations. Thus, the best combination of the controller parameters is obtained with a systematic hit-and-trial technique, and the parameters are given in the Appendix. It is emphasized that these controller parameters are not optimal and better parameters could be obtained by following more rigorous control-design techniques. However, the objective of this paper is only to demonstrate a new concept of using a PV solar farm inverter as an STATCOM using these reasonably good controller parameters. In this controller, although the line current magnitude signal is used, other local or remote signals, which reflect the generator rotor-mode oscillation, may also be utilized.

3.2 System Studies-II

Transient stability studies are carried out using PSCAD/ EMTDC simulation software, for both the study systems during night and day, by applying a three-line-to-ground (3LG) fault at bus 1 for five cycles. The damping ratio is used to express the rate of decay of the amplitude of oscillation.

Table 3: Power Flows And Voltages For Study System I For Solar Dg With Conventional Reactive Power Control And Proposed Damping Control Both During Nighttime And Daytime (1.05 P.U.)

Simulation Description		Gen. Bus	PCC/Middle Bus (3)			Inf. Bus
		Pg (MW)	Vpcc (pu)	Psolar (MW)	Qsolar (MVar)	Pinf (MW)
Nighttime	Conventional Operation of Solar DG	731	1.010	0	0	-708
	Solar DG with damping controller	850	1.000	-0.20	0.08	-819
Daytime	Conventional Operation of Solar DG	730	1.010	19.0	-0.50	-725
	Solar DG	719	1.008	91.0	-0.20	-786
	Solar DG with damping controller	851	1.000	19.0	-0.06	-839
	Solar DG with damping controller	861	0.994	91.0	-0.20	-917

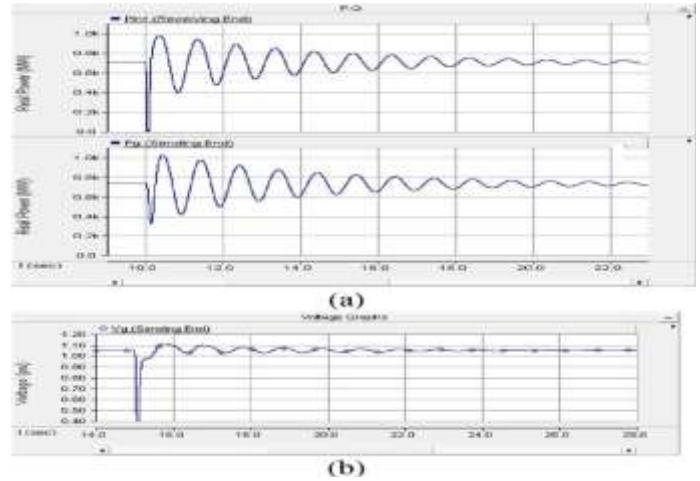


Figure 7: (a) Maximum nighttime power transfer (731 MW) from the generator when solar DG remains idle. (b) Voltage at the generator terminal.

Therefore, for a 5% damping ratio of the rotor mode having an oscillation frequency of 0.95 Hz, as considered in this study, the post fault clearance settling time of the oscillations to come within 5% (typically within 3 times the time constant) of its steady-state value is almost 10 s. The peak overshoot of PCC voltage should also be limited within 1.1 p.u. of nominal voltage. The maximum stable generator power limit for the system is determined through transient stability studies for different modes of operation of the solar DG in study system 1, and those of the solar DG and the solar/winds DGs in study system 2.

A. Case Study1: Power Transfer Limits in Study System 1

1) Conventional Reactive Power Control with Novel Damping Control:

In this study, the solar DG is assumed to operate with its conventional reactive power controller and the DG operates at near unity power factor. For the night time operation of solar DG, the dc sources (solar arrays) are disconnected, and the solar DG inverter is connected to the grid using appropriate controllers, as will be described. Power transmission limits are now determined for the following four cases. The stable power transmission limits obtained from transient stability studies and the corresponding load-flow results are presented in Table 4 where -ve **q** represents the inductive power drawn and represents the capacitive power injected into the network.

Solar DG Operation during Night with Conventional Reactive Power Controllers:

The maximum stable power output from the generator is 731 MW when the solar DG is simply sitting idle during the night and is disconnected from the network. This power-flow level is chosen to be

the base value of which the improvements in power flow with different proposed controllers are compared and illustrated later in Table 6. The real power from the generator and that entering the infinite bus for this fault study are shown in Fig. 7(a). The sending-end voltage at the generator is shown in Fig. 7(b) which shows a voltage overshoot of 1.1p.u.

Solar DG Operation during the Night with Damping Controllers:

The quantities are illustrated in Fig. 8(a). The damping controller utilizes the full rating of the DG inverter at night to provide controlled reactive power and effectively damps the generator rotor-mode oscillations.

The voltages at generator bus and at the PCC bus are depicted in Fig. 8(b). A very small amount of negative power flow from the solar farm is observed during night time.

This reflects the losses in the inverter IGBT switches as well as transformer and filter resistances by the flow of real current from the grid into the solar farm inverter to charge the dc-link capacitor and maintain its voltage constant while operating the PV inverter as STATCOM with the damping controller (or even with a voltage controller). During night time, the reference dc-link voltage is chosen around the typical daytime-rated maximum power point (MPP) voltage. The oscillations in the solar PV power output during night time, as seen in Fig. 8, are due to the active power exchanged by the solar inverter both during the charge and discharge cycles in trying to maintain a constant voltage across the dc-link capacitor, thereby enabling the inverter to operate as an STATCOM.

Solar DG Operation during the Day of a Conventional Reactive Power Controller:

The conventional control of a PV solar DG does not seem to alter the stable transmission limit in any appreciable manner.

Table 5: Power Flows And Voltages For Study System I For Solar Dg With The Proposed Pcc Voltage Control And Damping Control During Nighttime And Daytime (1.05p.U.)

Table 5: Increase In The Stable Power Transfer Limit (In Megawatts) For Study System I With Different PV-STATCOM Controls

PV STATCOM CONTROL	NIGHT	DAY	
		Solar Power Output 19 MW	Solar Power Output 91 MW
Voltage Control	102	85	7
Damping Control	119	121	142
Voltage Control with Damping Control	168	93	36

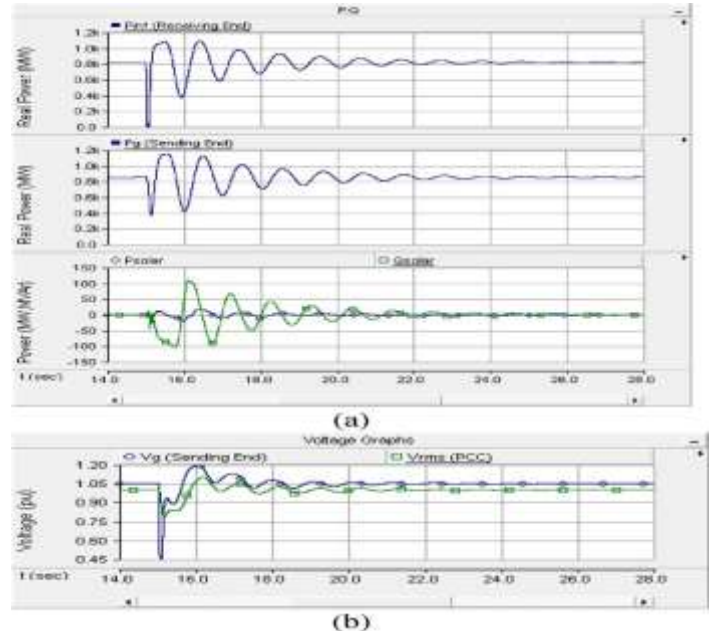


Figure 8: (a) Maximum night time power transfer (850 MW) from the generator with solar DG using the damping controller. (b) Voltages at the generator terminal and DG PCC.

Solar DG Operation during the Day with a Damping Controller:

The quantities and are shown for the cases without the damping controller and with the damping controller in Figs. 9 and 10, respectively.

The available inverter capacity after real power generation of 91 MW is 41.5 MVar, which is used for damping oscillations during the day. The power transfer capacity increase in the daytime is expected to be lower than the night time since only a part of the total inverter capacity is available for damping control during the day. However, it is noticed from Table 4 that the maximum power transfer during night time (850 MW) is actually less than the maximum power transfer value during the daytime (861 MW). This is because of an additional constraint that while increasing the power transfer, the overshoot in PCC voltage should not exceed 1.1 p.u. If the power transfer is allowed until Fig.9.

Maximum daytime power transfer (719 MW) from the generator with solar DG generating 91-Mits damping ratio limit of 5% regardless of voltage overshoot, the maximum night time power transfer is observed to be 964 MW whereas the maximum daytime power transfer is expectedly seen to be lower at 940 MW (plots not shown).

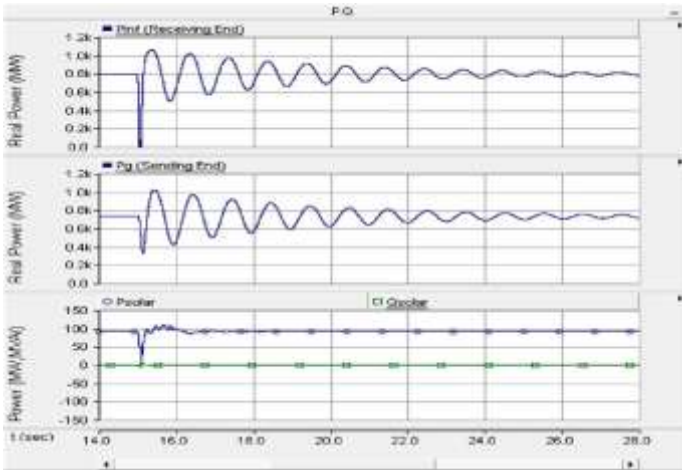


Figure 9: Maximum daytime power transfer (719 MW) from the generator with Solar DG generating 91-MW real power.

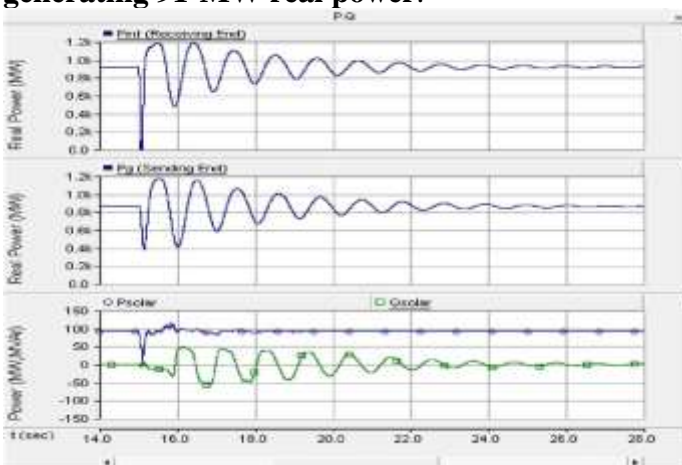


Figure 10: Maximum daytime power transfer (861 MW) from the generator with Solar DG generating 91-MW real power and using the damping controller

2) PCC Voltage Control with the Novel Damping Control:

Transient stability results for a new control strategy involving PCC voltage control, together with damping control, are shown in Table for the following four cases.

Solar DG Operation during the Night with a Voltage Controller:

The increase in the power transfer limit depends upon the choice of reference values for PCC voltage. In the best scenario when is regulated to 1.01 p.u., the maximum power output from the generator increases to 833 MW, compared to 731 MW when the solar DG operates with conventional reactive power control.

Solar DG Operation during the Day with the Voltage Controller:

The power transfer increases for both low (19 MW) and high (91 MW) power output from the solar farm are seen to be highly sensitive to the PCC bus voltage set point. It is also noted that with lower availability of reactive power capacity after real

power production, the ability to change the bus voltage is limited, which leads to a lower increase in power transmission capacity. Solar DG Operation during the Night with Both Voltage and Damping Controllers.

The generator and infinite bus power are depicted, and corresponding voltages are shown. Although the rotor-mode oscillations settle faster, the power transfer cannot be improved beyond 899 MW due to high overshoot in voltages

Solar DG Operation during the Day with Voltage and Damping Controllers:

A further increase in power transfer is observed when both voltage control and damping control are employed, compared to case 2) when only the voltage controller is utilized. For Study System 1, the net increase in power transfer capability as achieved with different PV-STATCOM controls in comparison with that obtained from conventional reactive power control of the solar DG is summarized in Table 5.

The maximum increase in the power transfer limit during night time is achieved with a combination of voltage control and damping control, whereas the same during daytime is accomplished with damping control alone. This is because, at night, the entire megavolt-ampere rating of the solar DG inverter is available for reactive power exchange, which can be utilized for achieving the appropriate voltage profile at PCC conducive for increasing the power transfer, as well as for increasing the damping of oscillations. During daytime, first, the generation of real power from the solar DG tends to increase the voltage at PCC and second, the net reactive power availability also gets reduced especially with large solar real power outputs. Therefore, it becomes difficult with the limited reactive power to accomplish the appropriate voltage profile at PCC for maximum power transfer and to impart adequate damping to the oscillations. However, if only damping limits appear to improve with higher real power outputs from the solar DG. This is because real power generation increases the PCC voltage which can be potentially helpful in increasing the power transfer capacity. Since damping control is found to be more effective during the daytime, the same is explored further for the following studies. Control is exercised during daytime, power transfer.

B. Case Study 2: Power Transfer Limits in Study System II

In this study, the proposed damping control strategy is compared with the conventional reactive power control strategy for Study System II shown in Fig.

5(b). A three-phase-to-ground fault of 5 cycles is applied to the generator bus at 8 s. The power transfer limits obtained through transient stability studies for different cases are illustrated in Table 6.

The following eight cases are studied:

Night-time:

Case 1 – None of the DGs Generate Real Power: The maximum power transfer limit is 731 MW as in Table 3.

Case 2 – Only Wind DG Generates Real Power. Both DGs Operate With Conventional Reactive Power Control: The power transfer limit decreases slightly with increasing wind power output.

Case 3 – None of the DGs Generate Real Power But Both DGs Operate With Damping Control:

The different variables, generator power, infinite bus power, real power of wind DG, reactive power of the wind DG, real power of the solar DG, and the reactive power of the solar DG Maximum night time power transfer from the generator with both DGs using the damping controller but with no real power generation are illustrated in Fig. 11. Even though the entire ratings (100 MVar) of the wind DG and solar DG inverters are not completely utilized for damping control, the power transfer limit increases significantly to 960 MW.

Case 4 – Only Wind DG Generates Real Power But Both DGs Operate on Damping Control: There is only a marginal improvement in the power limit with decreasing power output from the wind DG.

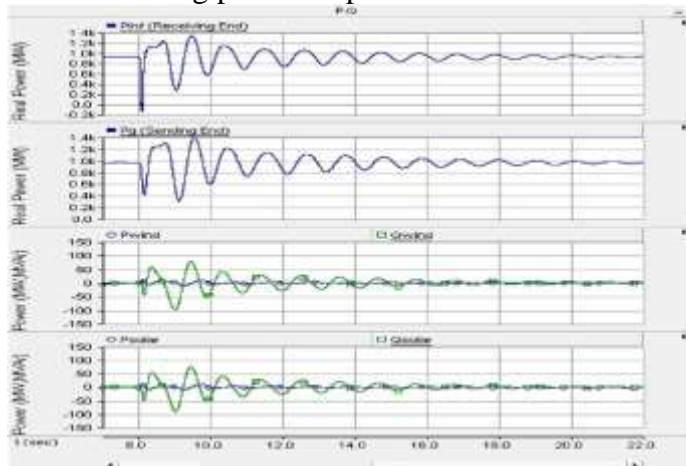


Figure 11: Maximum nighttime power transfer from the generator with both DGs

Using the damping controller but with no real power generation

Daytime:

Case 5 – Both DGs Generate Real Power: The power transfer limit from the generator decreases as the power output from both DGs increase.

Case 6 – Only Solar DG Generates Power: The power transfer limit from the generator decreases as the power output from the solar DG increases.

However, no substantial changes in power limits are observed compared to the case when both DGs generate power (Case 5).

Case 7 – Both DGs Generate Real Power and Operate on Damping Control: This case is illustrated by different variables and in Fig. 12. The power limit does not change much with increasing power output from both DGs.

Case 8 – Only Solar DG Generates Real Power But Both DGs Operate on Damping Control: The power limit does not appear to change much with increasing power output from the solar DG. For Study System 2, the net increases in power transfer limits accomplished with the proposed novel damping control for different real power outputs from both DGs compared to those attained with the conventional operation of both DGs, are depicted in Table 6. The proposed damping control on the two DGs (of rating 100 MW each) in the night increases the power transfer limits substantially by about 220 MW. This is expected since in the night, the entire inverter MVA rating of both DGs is available for damping control. The improvement is slightly less when wind DG produces high power. This is also expected as the reactive power availability decreases with the wind DG power output. During daytime, the proposed damping control on both DGs also increases the power transfer limits substantially. A greater increase is seen during high-power generation by any DG, since high power output improves the PCC voltage profile which assists in increasing the power transfer capacity

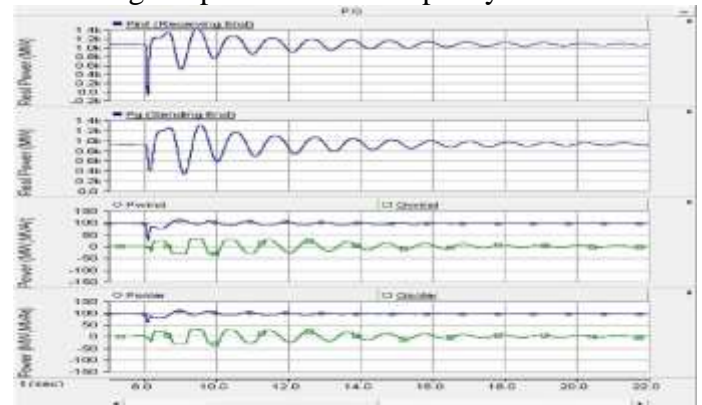


Figure 12: Maximum daytime power transfer from the generator while both DGs Generate 95 MW, each using a damping controller.

Table 6: Increase In Power Transfer Limits For Study System II

DG Real Power Outputs (MW)	Power Limit Increase (MW)
NIGHT	
$P_{\text{solar}} = 0; P_{\text{wind}} = 0$	229
$P_{\text{solar}} = 0; P_{\text{wind}} = 20$	219
$P_{\text{solar}} = 0; P_{\text{wind}} = 95$	220
DAY	
$P_{\text{solar}} = 20; P_{\text{wind}} = 20$	197
$P_{\text{solar}} = 95; P_{\text{wind}} = 95$	230
$P_{\text{solar}} = 20; P_{\text{wind}} = 0$	214
$P_{\text{solar}} = 95; P_{\text{wind}} = 0$	219

WITH DIFFERENT DG POWER OUTPUTS

3.3 IMPLEMENTATION OF PV-STATCOM ON LARGE-SCALE SOLAR SYSTEMS

The PV-STATCOM technology will be showcased for the first time in a utility network of Ontario on a 10-kW PV solar system. The 10-kW solar system will be utilized for voltage regulation and power factor correction in addition to generating real power.

Several detailed testing and validation studies are required to be completed before the PV-STATCOM will be allowed to connect to the wires of the utility. These include:

- 1) PV-STATCOM controller testing with PSCAD/EMTDC simulation studies;
- 2) Controller validation using real-time digital simulation (RTDS); and, finally,
- 3) a full-scale 10-kW lab-scale demonstration of the PV-STATCOM. Other lab tests would be performed to meet requirements of IEEE standard 1547.

The path for implementing PV-STATCOM technology in large real-scale solar power systems is much more complex than that for the 10-kW systems. Major issues have to examine and addressed the PV-STATCOM concept to different configurations of inverters: six-pulse, multi-pulse, multilevel, etc., and control coordination amongst multiple inverters in a PV solar plant, with each operating in PV-STATCOM mode, need to be addressed. Grid connection issues, such as protection and control, voltage rise and harmonics, short-circuit current limitations, disconnection during faults, or staying connected with low-voltage ride-through (LVRT) capabilities, need to be examined. Retro-fitting PV inverters in large solar plants with PV-STATCOM technology will have to deal with warranty issues of inverters, in addition to revalidation of the solar system performance with the new PV-STATCOM.

3.4 PRACTICALITY OF UTILIZING LARGE-SCALE SOLAR FARMS FOR ENHANCING TRANSMISSION LIMITS

The number of large solar farms is increasing worldwide. There are at least four operating solar farms of 100-MW rating, three of which are

connected at transmission-level voltages with more to follow. The 550-MW Desert Sunlight Solar Farm Project in California will connect to California's existing 500-kV transmission grid. The Grand Renewable Energy Park, ON, Canada, has a 100-MW solar farm connected to the 230-kV transmission line. Meanwhile, several new transmission lines are being constructed worldwide to enhance power transfer capacity in transmission corridors. Examples of new lines for carrying power from renewable sources are the SWIP project, CREZ initiative, and BPA system. Evidently, these new lines are being constructed due to inadequate power transfer capacity in these corridors. There is therefore a potential opportunity for large-scale solar farms connected to such lines.

4. SIMULATION AND RESULTS

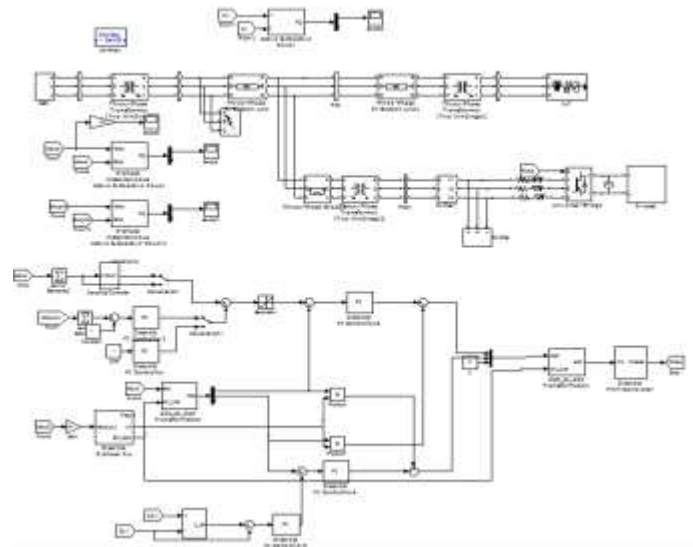


Figure 13: Proposed simulation diagram of PV-STATCOM

4.1 Maximum nighttime power transfer (731 MW) from the generator When solar DG remains idle

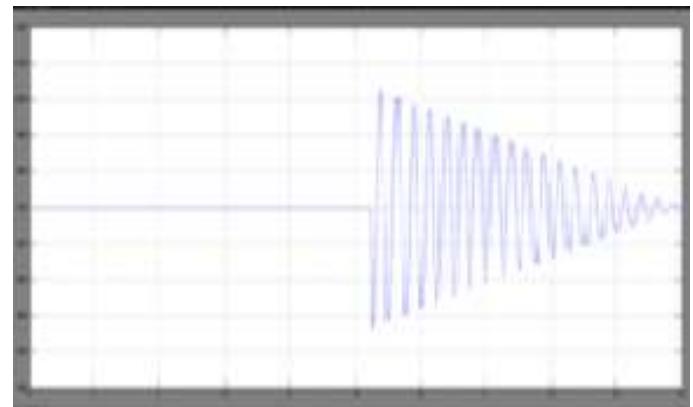


Figure 14: Real power at receiving end.

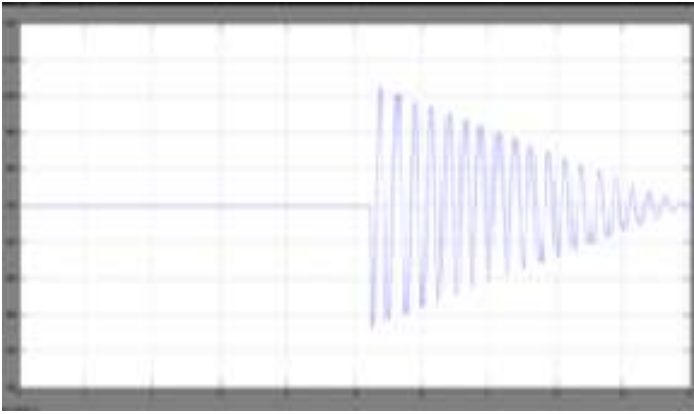


Figure 15: Real power at sending end.

4.2 Maximum nighttime power transfer (850 MW) from the generator with Solar DG using the damping controller

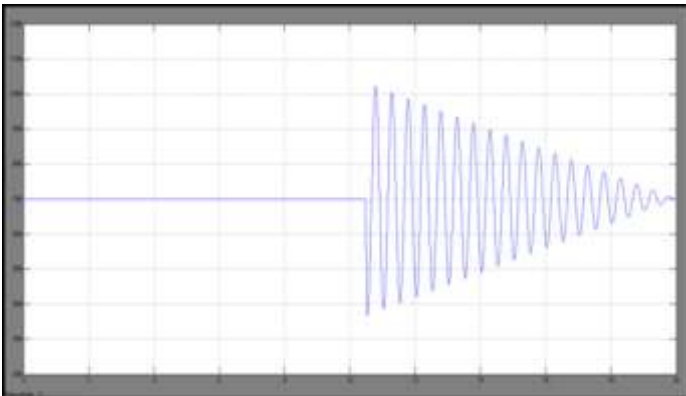


Figure 16: Real power at sending end (850) MW

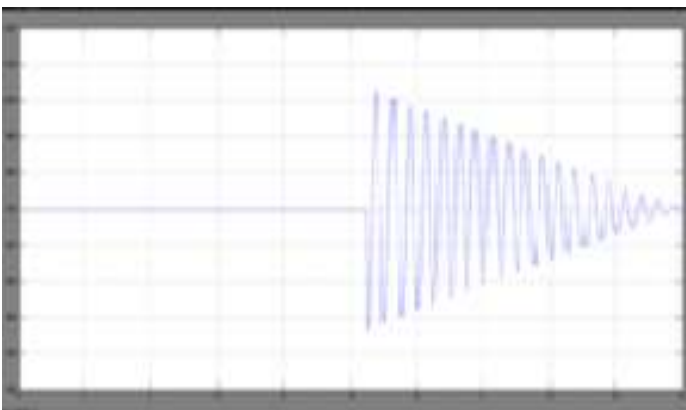


Figure 16: Real power at receiving end.

4.3 Maximum daytime power transfer (719 MW) from the generator with Solar DG generating 91-MW real power

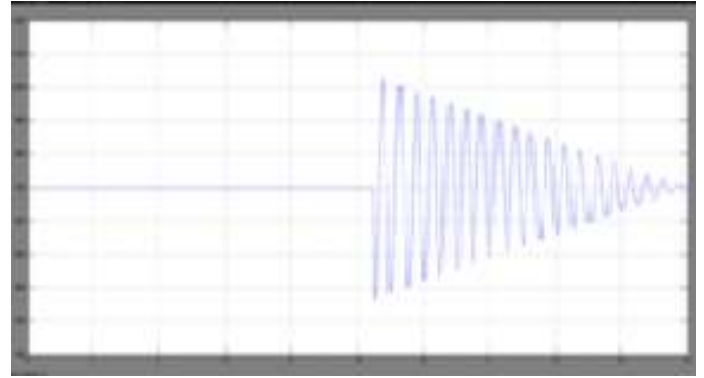


Figure 17: Real power at receiving end

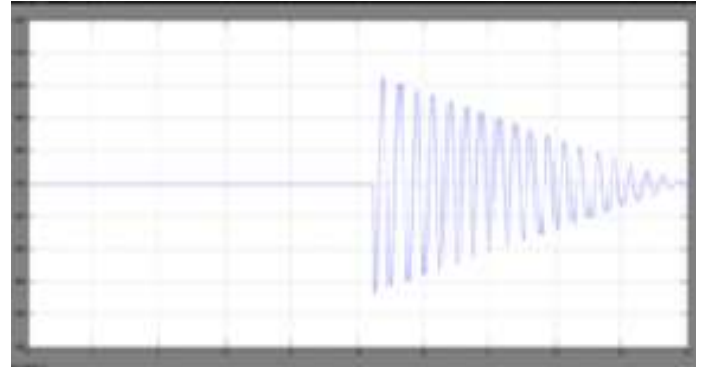


Figure 18: Real power at sending end

5. CONCLUSION

Solar farms are idle during nights. A novel patent-pending control paradigm of PV solar farms is presented where they can operate during the night as an STATCOM with full inverter capacity and during the day with inverter capacity remaining after real power generation, for providing significant improvements in the power transfer limits of transmission systems. This new control of PV solar system as STATCOM is called PV-STATCOM. The effectiveness of the proposed controls is demonstrated on two study SMIB systems: System I have one 100-MW PV-STATCOM and System II has one 100-MW PV-STATCOM and another 100-MW PV-STATCOM or 100-MW wind farm controlled as STATCOM. Three different types of STATCOM controls are proposed for the PV solar DG and inverter-based wind DG. These are pure voltage control, pure damping control, and a combination of voltage control and damping control. The following conclusions are made: 1) In study system I, the power transfer can be increased by 168 MW during night time and by 142 MW in the daytime even when the solar DG is generating a high amount of real power. 2) In Study System II, the transmission capacity in the night can be increased substantially by 229 MW if no DG is producing real power. During night time and daytime, the power transfer can be increased substantially by 200 MW, even when the DGs are

generating high real power. This study thus makes a strong case for relaxing the present grid codes to allow selected inverter-based renewable generators (solar and wind) to exercise damping control, thereby increasing much-needed power transmission capability. Such novel controls on PV solar DGs (and inverter-based wind DGs) will potentially reduce the need for investments in additional expensive devices, such as series/shunt capacitors and FACTS. The PV-STATCOM operation opens up a new opportunity for PV solar DGs to earn revenues in the night time and daytime in addition to that from the sale of real power during the day. This will, of course, require appropriate agreements between the regulators, network utilities, solar farm developers, and inverter manufacturers.

6. REFERENCES

- [1] Varma, Rajiv K., Shah Arifur Rahman, and Tim Vanderheide. "New control of PV solar farm as STATCOM (PV-STATCOM) for increasing grid power transmission limits during night and day." *IEEE transactions on power delivery* 30.2 (2015): 755-763.
- [2] Rajasekharachari, K., G. Balasundaram, and K. Kumar. Implementation of A Battery Storage System of An Individual Active Power Control Based on A Cascaded Multilevel PWM Converter. *Int J Inno Res Sci Eng Technol.* 2013; 2(7).
- [3] Kumar K, S.V. Sivanagaraju, Rajasekharachari. Single Stage AC-DC Step Up Converter using Boost And Buck-Boost Converters. *Int J Adv Res Electric Electron Instru Eng.* 2013; 2(9): 4245-4252.
- [4] Varma, Rajiv K., and Reza Salehi. "SSR Mitigation With a New Control of PV Solar Farm as STATCOM (PV-STATCOM)." *IEEE Transactions on Sustainable Energy* (2017).
- [5] Nivedha, R., R. Narmatha Banu, and A. Om Prakash. "Enhancement of grid power transmission limits using photovoltaic solar farm as STATCOM (PV-STATCOM)." *Computing Technologies and Intelligent Data Engineering (ICCTIDE), International Conference on.* IEEE, 2016.
- [6] Cabrera-Tobar, Ana, et al. "Review of advanced grid requirements for the integration of large scale photovoltaic power plants in the transmission system." *Renewable and Sustainable Energy Reviews* 62 (2016): 971-987.
- [7] Maleki, Hesamaldin, and Rajiv K. Varma. "Coordinated control of PV solar system as STATCOM (PV-STATCOM) and Power System Stabilizers for power oscillation damping." *Power and Energy Society General Meeting (PESGM), 2016.* IEEE, 2016.
- [8] Al Awadhi, Nada, and Mohamed Shawky El Moursi. "A Novel Centralized PV Power Plant Controller for Reducing the Voltage Unbalance Factor at Transmission Level Interconnection." *IEEE Transactions on Energy Conversion* 32.1 (2017): 233-243.
- [9] Kumar, K., N. Ramesh Babu, and K. R. Prabhu. "Design and Analysis of an Integrated Cuk-SEPIC Converter with MPPT for Standalone Wind/PV Hybrid System." *International Journal of Renewable Energy Research (IJRER)* 7.1 (2017): 96-106.
- [10] S. V. Sivanagaraju, K. Kumar, K. Rajasekharachari. Performance Comparison Of Variable Speed Induction Machine Wind Generation System With And Without Fuzzy Logic Controller. *Int J Innov R Devel.* 2013; 2(7).
- [11] Hussain, Ikhlaiq, Maulik Kandpal, and Bhim Singh. "Grid integration of single stage SPV-STATCOM using cascaded 7-level VSC." *International Journal of Electrical Power & Energy Systems* 93 (2017): 238-252.
- [12] Rajasekharachari, K., and K. Shalini, Kumar. K and SR Divya. Advanced Five Level-Five Phase Cascaded Multilevel Inverter with SVPWM Algorithm. *Int J Electric Engi & Technol.* 2013; 4(4): 144-158.
- [13] Choi, Dong-Hee, et al. "Analysis on Special Protection Scheme of Korea Electric Power System by Fully Utilizing STATCOM in a Generation Side." *IEEE Transactions on Power Systems* 32.3 (2017): 1882-1890.
- [14] Yang, Hong-Tzer, and Jian-Tang Liao. "Hierarchical reactive power regulation strategies for high-penetration photovoltaic distribution systems." *International Journal of Energy Research* 40.3 (2016): 332-342.
- [15] Benyahia, Khaled, et al. "Dynamic performance enhancement of Doubly fed induction generator-based wind farm using photovoltaic solar farm as STATCOM." *Electrical Engineering (ICEE), 2015 4th International Conference on.* IEEE, 2015.